Impact of a narrow limiter SOL heat flux channel on the ITER first wall panel shaping

IOP Publishing | International Atomic Energy Agency Nuclear Fusion
Nucl. Fusion 55 (2015) 033019 (16pp) doi:10.1088/0029-5515/55/3/033019

Impact of a narrow limiter SOL heat flux channel on the ITER first wall panel shaping

M. Kocan[1], R.A. Pitts[1], G. Arnoux[2], I. Balboa[2], P.C. de Vries[1], R. Dejarnac[3], I. Furno[4], R.J. Goldston[5], Y. Gribov[1], J. Horacek[3], M. Komm[3], B. Labit[4], B. LaBombard[6], C.J. Lasnier[7], R. Mitteau[1], F. Nespoli[4], D. Pace[8], R. Panek[3], P.C. Stangeby[9], J.L. Terry[6], C. Tsui[9] and P. Vondracek[3]

[1] ITER Organization, Route de Vinon-sur-Verdon CS 90 046, F-13067 St Paul lez Durance Cedex, France
[2] JET-EFDA, Culham Science Centre, Abingdon, OX14 3DB, UK
[3] Institute of Plasma Physics, ASCR v.v.i., Za Slovankou 3, 182 00 Prague, Czech Republic
[4] Ecole Polytechnique Fédérale de Lausanne, Centre de Recherches en Physique des Plasmas, 1015 Lausanne, Switzerland
[5] Princeton Plasma Physics Laboratory, Princeton, NJ 08543, USA
[6] MIT PSFC, 175 Albany Street, Cambridge, MA 02139, USA
[7] Lawrence Livermore National Laboratory, 7000 East Avenue, Livermore, CA 94550, USA
[8] General Atomics, PO Box 85608, San Diego, CA 92186-5608, USA
[9] University of Toronto Institute for Aerospace Studies, Toronto, M3H 5T6, Canada

E-mail: martin.kocan@iter.org

Received 28 October 2014, revised 15 January 2015
Accepted for publication 3 February 2015
Published 27 February 2015

Abstract

The inboard limiters for ITER were initially designed on the assumption that the parallel heat flux density in the scrape-off layer (SOL) could be approximated by a single exponential with decay length λ_q. This assumption was found not to be adequate in 2012, when infra-red (IR) thermography measurements on the inner column during JET limiter discharges clearly revealed the presence of a narrow heat flux channel adjacent to the last closed flux surface. This near-SOL decay occurs with $\lambda_q \sim$ few mm, much shorter than the main SOL λ_q, and can raise the heat flux at the limiter apex a factor up to ∼4 above the value expected from a single, broader exponential. The original logarithmically shaped ITER inner wall first wall panels (FWPs) would be unsuited to handling the power loads produced by such a narrow feature. A multi-machine study involving the C-Mod, COMPASS, DIII-D and TCV tokamaks, employing inner wall IR measurements and/or inner wall reciprocating probes, was initiated to investigate the narrow limiter SOL heat flux channel. This paper describes the new results which have provided an experimental database for the narrow feature and presents an ITER inner wall FWP toroidal shape optimized for a double-exponential profile with $\lambda_q = 4$ (narrow feature) and 50 mm (main-SOL), the latter also derived from a separate multi-machine database constituted recently within the International Tokamak Physics Activity. It is shown that the new shape allows the power handling capability of the original shape design to be completely recovered for a wide variety of limiter start-up equilibria in the presence of a narrow feature, even taking assembly tolerances into account. It is, moreover, further shown that the new shape has the interesting property of both mitigating the impact of the narrow feature and resulting in only a very modest increase in heat load, compared to the current design, if the narrow feature is not eventually found on ITER.

Keywords: ITER, limiter plasma, heat flux density, scrape-off layer, first wall panels, narrow feature

(Some figures may appear in colour only in the online journal)

1. Introduction

In ITER, as in many divertor tokamaks, the plasma will start (and terminate) in a limiter configuration, leaning either on the inner wall (IW) or on the outer wall (OW), before the X-point is established. Following the elimination of a pair of discrete OW limiters after the ITER First Wall Design Review in 2007, the start-up limiters in ITER now comprise both, the IW and the OW first wall panels (FWPs) adjacent to the tokamak equatorial plane [1, 2]. Designing these FWPs so that they withstand the power fluxes expected during the plasma start-up presents a daunting engineering challenge [3]. The FWP must be shaped toroidally to ensure that any misalignments which occur from panel to panel (a maximum of 5 mm is called for in the ITER first wall design) do not present leading edges to plasma impact.

Any introduction of shaping implies concentration of power with respect to a perfectly cylindrical surface. In order to spread the incident heat flux as uniformly as possible over the plasma-wetted area and thus reduce the peak surface heat load, q_{peak}, the OW and, until recently, also the IW FWPs in ITER were given a logarithmic toroidal profile. When the parallel heat flux profile, $q_{\parallel}$, can be approximated by a single exponential, then a logarithmic toroidal profile limiter is nearly optimal for distributing the power load. The initial limiter design for ITER used a database of reciprocating Langmuir probe (RCP) measurements made on JET [4] and on Tore Supra [5]. These experiments used IW limiters and RCPs inserted at the top and somewhat to the low field side (LFS) of the poloidal cross-section. The measured radial profiles of the electron density, n_e, and temperature, T_e were consistent with a single exponential profile across the scrape-off layer (SOL), although little data were available very close to the last closed flux surface (LCFS). In 2010, ITER initiated further IW limiter studies on the Tore Supra, DIII-D and JET tokamaks to generate a more comprehensive database. This study again involved RCPs at the top and LFS and again found the SOL radial profiles to be approximately exponential [2, 6–9].

In 2012, observations at JET using infra-red (IR) thermography directly on the inner column of IW limited (IWL) discharges revealed the presence of a very narrow feature in the $q_{\parallel}$ profile, localized near the LCFS [10]. Motivated by the JET IR observations, the ITER Organization (IO) initiated a further multi-machine study of IW limiters—on the C-Mod, COMPASS, DIII-D and TCV tokamaks—this time including IW RCPs and/or IR measurements of the IW [11–14]. From these new studies, reviewed here, there is now ample evidence that $q_{\parallel}$ in IWL discharges does feature a narrow heat flux channel in the 'near-SOL' adjacent to the LCFS. This near-SOL decay occurs with $\lambda_q \sim$ few mm, much shorter than the main SOL λ_q, and can raise the heat flux at the limiter leading edge significantly above the value expected from a single, broader exponential profile for which the IW FWPs were originally designed.

In retrospect it is now clear that the JET observations have some similarities with narrow features seen earlier in pioneering studies with limiter plasmas on T-10 [15], TFTR [16], Tore Supra [17], TEXTOR [18, 19], and C-Mod [20], although, as will be discussed below in section 4, the relevance to the ITER IWL is not entirely clear. It is unfortunate that these early clues were not more thoroughly investigated when the original IW FWP toroidal profile was specified at the beginning of the Design Review activities which followed shortly after the IO was established.

The paper is organized as follows: section 2 focuses on selected aspects of the plasma start-up in ITER, important for the present study. Section 3 recalls some design features of the ITER FWPs. Section 4 summarizes recent experimental observations of the narrow near-SOL heat flux channel in IWL discharges, which constitute the new physics basis for the shaping design of the IW FWPs. Surface heat loads on the modified IW FWP in the presence as well as in the absence of the narrow feature, including the effect of the first wall assembly errors, are examined in section 6. A summary is provided in section 7.

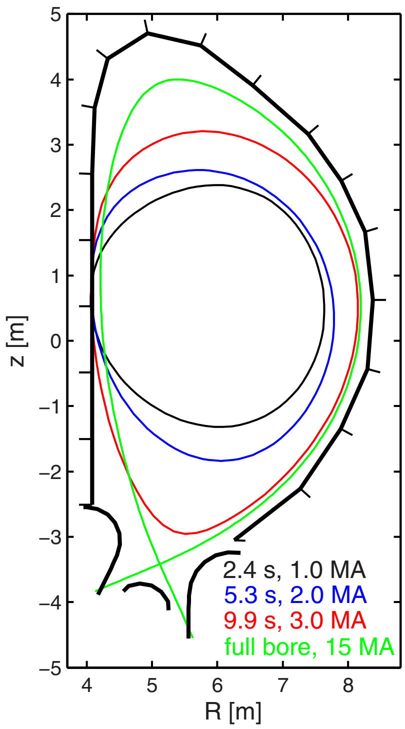

Figure 1. Example of ITER start-up on the IW obtained from a DINA code full scenario simulation [21].

2. Plasma start-up in ITER

In order to minimize the flux consumption in the limiter phase, ITER plasma scenario designs for burning plasma operation seek an X-point transition as early as possible in the current ramp-up (see figure 1). There are, however, a number of issues related to early X-point formation. Small variations in plasma initiation due to machine conditions can yield varying rates of plasma current increase following breakdown. This in turn may affect plasma radial position and internal inductance which can drive variations in plasma position and shape. As a result, inter-shot differences are expected to occur in both formation time of the X-point and the value of plasma current, I_p at that time.

In ITER, scenario design shows that a transition to X-point at $I_p \lesssim 3.5$ MA (corresponding to an edge safety factor at the LCFS, $q_{LCFS} \sim 10$) cannot be guaranteed systematically in each discharge due to possible saturation of voltage in the convertors of some coil power supplies which may cause degradation of plasma position and shape control. Indeed, circular limiter plasmas are required for vertical stability (using feedback on vertical position and major radius) up to $I_p \sim 1.5$ MA before elongation to full bore limiter configurations can begin with vertical stabilization active [21]. In general, due to the uncertainties in plasma inductance which may arise during the ramp-up to currents compatible with divertor formation (as a result of proximity to power supply voltage saturation, errors expected in the measurement of plasma–wall gaps and in the magnetic reconstruction at low current), it is not possible to guarantee a pure inboard or pure outboard plasma start-up. There are, however, several reasons why IW start-up on ITER is favoured: 3D stray fields produced by currents (which can be up to 1.5 MA during ramp-up) induced in the

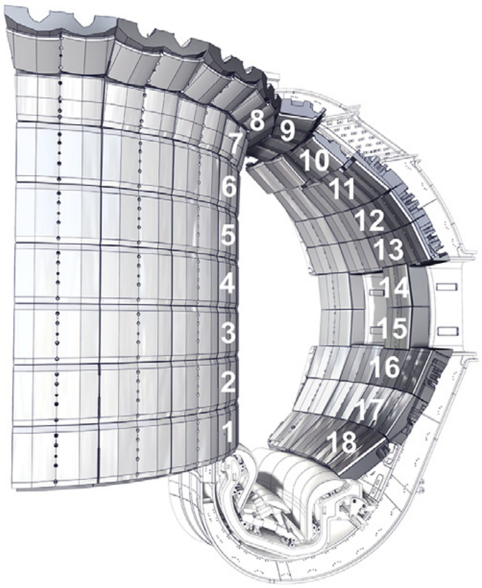

Figure 2. Portion of the ITER first wall with the FWP poloidal row reference numbers used in the text.

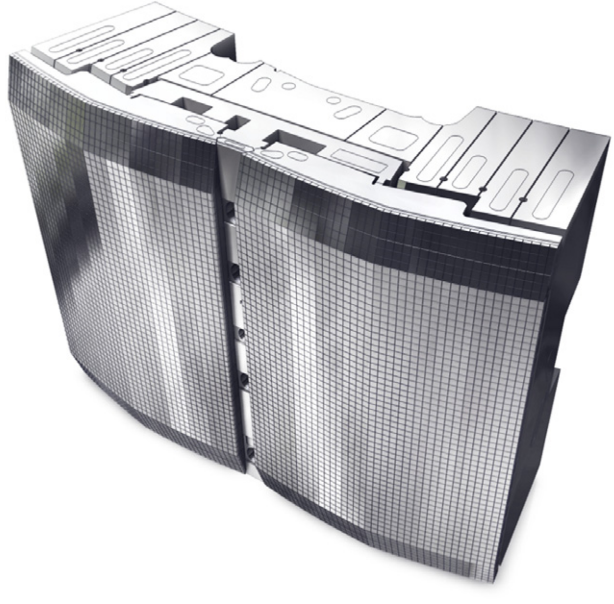

Figure 3. ITER IW FWP (poloidal row 4) mounted on its shield block. The approximate dimensions are $1.4 \times 1 \times 0.5$ m.

vacuum vessel are lower; the electron cyclotron resonance heating system which will be used for ITER plasma start-up assist has a resonance location towards the inboard side; and IW start-up maintains the plasma at a greater distance from the OW, where stray fields are higher due to the presence of port openings and ferritic inserts for toroidal magnetic field ripple minimization.

The ITER Heat Load Specifications, which are the design basis for all in-vessel components, prescribe that the IW and OW FWPs must tolerate steady state limiter operation at plasma currents as high as 7.5 MA, with the latter expected mostly during the ramp-down phases, mostly on the OW. For ramp-up, most scenarios will divert the plasma before $I_p \lesssim 5$ MA though the Heat Load Specifications maintain the 7.5 MA for all FW panels acting as limiters during ramp-up and down. These currents are associated with a power entering the SOL, P_{SOL} (MW) $\approx I_p$ (MA) [2] to allow for the use of some moderate level of additional heating (for example during plasma current ramp-up). In fact, as will be discussed later (section 6.1), if this equivalence of P_{SOL} and I_p is assumed, the actual value of I_p is unimportant and λ_q completely determines the parallel heat flux. However, the plasma wetted area and, more importantly the field line pitch angle depend on the ratio of poloidal to toroidal field and hence on the value of I_p.

3. IW and OW FWPs

Figure 2 shows a portion of the ITER first wall, illustrating how it is tiled using modular FWPs attached to massive shield blocks. As illustrated in figure 3, each FWP consists of a double-winged structure in the toroidal direction symmetrically disposed about a central, poloidally running slot which provides space for mechanical and hydraulic connections as well as for various plasma diagnostic systems [3, 22]. The toroidal circumference of both the IW and OW is formed by 18 FWPs, thus comprising 36 toroidal limiters, interrupted on the OW by diagnostic ports. For the start-up plasma configurations anticipated on ITER, appreciable heat loads are anticipated on the toroidal rows at poloidal locations 3–5 (IW start-up) and 14–15 (OW start-up). These FWPs are constituted of poloidal rows of separate toroidal fingers, each carrying small beryllium (Be) tiles (of dimension ~12 mm on a side and thickness in the range 6–8 mm) bonded to a CuCrZr hypervapotron heat sink and are rated to a peak steady-state surface heat flux density, $q_{peak}^{design} = 4.7\,\mathrm{MW\,m^{-2}}$ [3, 22]. These particular FWPs are dubbed 'enhanced heat flux' (EHF) panels to distinguish them from the 'normal heat flux' (NHF) units which feature a different cooling system and are designed for $q_{peak}^{design} = 2\,\mathrm{MW\,m^{-2}}$. On the IW, NHF panels are located at poloidal locations 1, 2 and 6. The EHF panel temperature equilibration time constant, $\tau \approx 2$–3 s is significantly shorter than the anticipated start-up duration (section 2), so that the FWPs are effectively exposed to a steady-state heat load during the start-up.

The original design basis for the FWP toroidal shaping was the incorporation of a logarithmic profile (approximated by a series of straight line segments, each carrying a series of smaller tiles), optimized for the handling of an exponential radial profile of parallel heat flux, $q_\parallel$ in the SOL [23]. The decay lengths are fixed differently for the IW and OW (with the local values $\lambda_{q,IW}^{design} = 50$ mm and $\lambda_{q,OW}^{design} = 15$ mm), originally on the basis of limited measurements available from L-mode divertor plasmas in a small number of tokamaks, but recently confirmed by a very extensive multi-machine database from which new scalings for ITER limiter start-up have been derived [24]. As explained in [23], for the purposes of the ITER design specification, the smallest expected λ_q values at the maximum permitted I_p are used to select $\lambda_{q,OW}^{design}$. The difference between $\lambda_{q,IW}^{design}$ and $\lambda_{q,OW}^{design}$ is due to strong outward ballooning transport near the outboard midplane (OMP) which is always observed on tokamaks. In the OW limited (OWL) configuration, the limiter suppresses the enhanced radial outward convection, leading to a narrow SOL, whilst in the

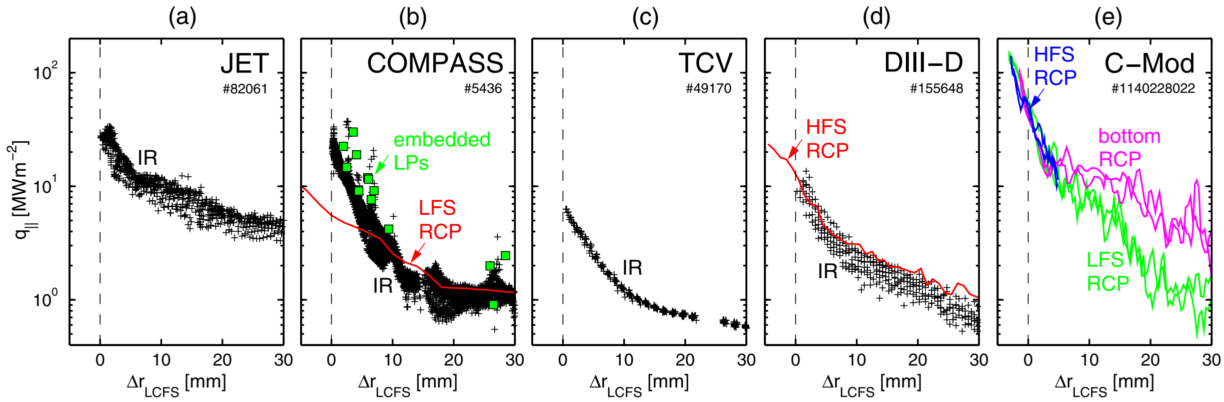

Figure 4. Radial profiles of $q_{\|}$ measured by IR and Langmuir probes in the IWL plasmas in different experiments [10–14, 30]. Profiles are mapped to the OMP.

IWL configuration, the plasma is allowed to expand freely on the outboard side, leading to a broad SOL ([5–7, 9, 25–28] and references therein).

In addition to surface heat loads which arise purely from the Heat Load Specifications (once the toroidal shaping is factored in), there are a number of 'add-on' penalty factors which must be accounted for to estimate the real expected worst case power loads [29]. These factors arise mainly due to probabilistic combination of assembly errors, as well as due to the FWP facets which can be seen in figure 3 (groups of flat Be tiles brazed to the same planar CuCrZr support). For example, for the maximum IW start-up plasma current with $P_{SOL} = 7.5$ MW and $\lambda_{q,IW} = \lambda^{design}_{q,IW}$, $q_{peak} = 3.4$ MW m^{-2} accounting for penalty factors [29], to be compared with the 'baseline' value of 2 MW m^{-2} if the penalties are not included. This is still well within (by ∼30%) the margins for steady state power handling on the EHF panels.

4. Narrow limiter SOL power channel

In the process of constituting a new multi-machine database of IWL λ_q measurements in order to consolidate the ITER scaling for $\lambda^{design}_{q,IW}$, observations at JET using IR thermography directly on limiter surfaces revealed the presence of a very narrow feature in the SOL heat flux density profile, localized near the LCFS ([10] and figure 4(*a*)). This near-SOL feature raises $q_{\|}$ at the limiter apex significantly above the value which would be extrapolated from the main-SOL heat flux density profile, which retains the classic broad exponential character assumed for the ITER toroidal FWP shaping design. The JET measured $q_{\|}$ profiles can be approximated by a double exponential consisting of two heat flux channels: the 'main-SOL' component, $q_{\|,main}$, with e-folding length $\lambda_{q,main}$ (corresponding to the $q_{\|}$ and λ_q of section 3), and the additional 'near-SOL' heat flux channel, $q_{\|,near}$, featuring an e-folding length $\lambda_{q,near} \ll \lambda_{q,main}$, but carrying an appreciable fraction of P_{SOL}:

$$q_{\|} = q_{\|,main} + q_{\|,near} = q_{\|0,main}\, e^{-\frac{\Delta r_{LCFS}}{\lambda^{OMP}_{q,main}}} + q_{\|0,near}\, e^{-\frac{\Delta r_{LCFS}}{\lambda^{OMP}_{q,near}}}, \quad (1)$$

with Δr_{LCFS} the radial distance from the LCFS and

$$q_{\|0,main} = \frac{P_{SOL}}{4\pi R_{OMP}\left(\lambda^{OMP}_{q,main} + R_q \lambda^{OMP}_{q,near}\right)\left(\frac{B_p}{B_{total}}\right)_{OMP}}, \quad (2)$$

evaluated from simple power balance at the OMP with

$$R_q \equiv q_{\|0,near}/q_{\|0,main}, \quad (3)$$

where the subscript '0' indicates the heat flux densities at the LCFS, and R_{OMP} and $(B_p/B_{total})_{OMP}$ are respectively the major radius and the magnetic field pitch angle at the OMP. Note that in the absence of the narrow feature ($R_q = 0$), equation (2) reduces to the usual power balance expression for single exponential $q_{\|}$ (e.g. equation (2) in [6]).

The JET experiments found $R_q = 1$–6 and $\lambda^{OMP}_{q,near} = 2$–4 mm, meaning that $q_{\|}$ near the limiter leading edge is strongly dominated by $q_{\|,near}$. On the other hand, no narrow component was found in the SOL ion current density profile measured in IWL discharges using a fast RCP entering the plasma in the upper LFS region of the poloidal cross-section [9]. One implication of this finding is that the narrow heat flux component is caused by the steepening of the radial energy flux rather than the particle flux, as observed earlier in C-Mod [20] (and ignoring potential instrumental effects linked to the use of the RCP—see last paragraph of this section).

The Introduction has alluded to the fact that with hindsight, it is now clear that the JET IR observations have some similarities with narrow heat flux features seen previously on limiter machines, notably in studies on T-10 [15], TFTR [16], Tore Supra [17], TEXTOR [18, 19], and C-Mod [20]. However, the relevance to the particular case of the ITER IWL is not entirely clear (in contrast to the more recent JET observations) [10]. Some of these previous experiments involved limiter geometries and locations significantly different from the ITER IWL. In particular, some involved very small impact angles near the contact point, making it unclear if the observed enhanced power deposition was due to a narrow $q_{\|}$ component only or to some cross-field effect. The uncertainty in the location of the LCFS is generally comparable to or greater than the radial extent of the narrow feature, necessitating systematic multi-machine studies to reach the definitive conclusions needed for engineering design decisions. The earlier studies were somewhat disparate in this sense. It is, nevertheless, unfortunate that these early clues were not more thoroughly investigated earlier on in the ITER IWL shaping design activities.

It was thus only after this much more recent JET experiment that it became obvious that the ITER IW would be unsuited to handling limiter power loads if a narrow heat flux feature were to be present. It is important to note here that the narrow feature observed in IWL discharges is not expected to affect the shape of the ITER OW FWPs, for which $\lambda_{q,OW}^{design}$ is already very short due to the aforementioned poloidal asymmetry in the radial particle and energy transport. This inherently short $\lambda_{q,OW}$ (though not as short as $\lambda_{q,near}$) makes the narrow heat flux feature observed in the IWL plasmas hard to discern in the OWL discharges. A very striking demonstration of this can be seen in figure 1 of [10].

Even though the JET observations of the narrow heat flux feature placed a serious question mark over the assumption of a single exponential heat flux profile in the IW limiter SOL, extrapolation to ITER on the grounds of a single experimental result is clearly unsatisfactory, particularly in view of the modifications it would imply to the FWP shaping. It is not, for example, clear what scaling to apply for $\lambda_{q,near}$ for ITER, with a factor 2 higher major radius and which will operate at higher I_p in limiter plasmas than was achieved in the JET experiment. Moreover, with only a single experiment on a single device, it is not possible to exclude the influence of limiter geometry on the presence of a narrow feature, especially if the feature is not also found (as on JET) in the SOL ion flux profile (JET has 16 discrete IW poloidal belt limiters separated by 0.75 m toroidally, ITER has 18 IW panels with 36 discrete limiter apexes).

As a result of the JET experiments, a multi-machine experimental effort was initiated to study this IWL physics and to attempt to provide a sufficiently robust basis to make a recommendation for an adjustment to the ITER IW FWP shape. Together with the JET data, this effort now includes measurements from five tokamaks covering a wide range of potential scaling parameters ($R = 0.5$–3 m, $I_p = 0.1$–2 MA and $q_{LCFS} = 2$–9). A brief summary of the results of these experiments is given here in order to provide a basis for the extrapolation to ITER which is required for the IW FWP toroidal shape analysis presented in section 5. Full details of the individual experiments may be found in [11–14]. Figure 4 gathers representative $q_\parallel$ profiles from all five experiments.

4.1. COMPASS

In an attempt to unravel the physics controlling the narrow feature, special IW limiters with various toroidal profile shapes were installed in the COMPASS tokamak and exposed to a large number of IWL discharges with different combinations of I_p and toroidal magnetic field (B_t) directions [12]. The steepening of $q_\parallel$ in the near SOL was observed systematically using IR thermography observing the limiter [12] and embedded Langmuir probes [11] (figure 4(*b*)). In the majority of cases, however, $q_\parallel$ profiles inferred from RCP systems entering the SOL from the top and at the OMP did not exhibit a narrow feature and can be reasonably approximated by single exponentials ([12] and figure 4(*b*)). In COMPASS, the IR-inferred $R_q \approx 2$–3 on average when the special limiter was radially aligned with toroidal neighbours and $R_q \approx 5$ on average when the limiter was inserted into the plasma by 8 mm compared to the nominal IW radius. One of the limiter toroidal shapes studied featured a variant optimized to spread the surface heat load, q_{surf} more uniformly in the presence of the narrow feature. In this case, the peak q_{surf} was observed further away from the limiter apex, demonstrating that the narrow feature is not caused by heat attraction or direct cross-field diffusion to the limiter leading edge as speculated in [10], but rather by a steepening of $q_\parallel$ in the near SOL. In COMPASS, $\lambda_{q,near}^{OMP} = 2$–$8$ mm, with $\lambda_{q,main}$ still consistent with the recent multi-machine scaling [24].

4.2. TCV

The narrow feature has also been found using IR thermography in plasmas limited on a central column consisting of 32 rounded graphite tiles, similar in number to the 36 limiters in ITER. The TCV data yield $R_q = 2$–4 and $\lambda_{q,near}^{OMP} = 1$–$3$ mm ([13] and figure 4(*c*)). About 25% of q_{surf} measured near the plasma contact point (where the field line incidence angle $\alpha_{inc} \to 0$) has been associated with direct cross-field transport operating according to a ‘funnel’ type effect [16].

4.3. DIII-D

On DIII-D, high-field-side (HFS) RCP and IR measurements have also clearly observed the narrow feature in IWL plasmas ([14] and figure 4(*d*)). As in COMPASS, no clear evidence was found for the narrow heat flux channel from the bottom and OMP RCPs in DIII-D. The average $R_q \approx 1$ (with $\lambda_{q,near}^{OMP} = 2$–$5$ mm) is also smaller compared to other experiments. One potential explanation for this behaviour might be the toroidally more symmetric IW in DIII-D (48 apexes), which leads to a toroidally more uniform power loading.

4.4. C-Mod

The most recent set of measurements in the multi-machine effort to understand the narrow heat flux feature has been obtained on C-Mod (figure 4(*e*)), on this occasion using only RCP systems (OMP, HFS and bottom of the plasma cross-section). Unlike in the four other tokamaks, the narrow feature is clearly found on C-Mod with LFS Langmuir probe measurements. First experiments found $R_q \approx 2$–4 and $\lambda_{q,near}^{OMP} = 1$–$2$ mm [30]. It is worth reiterating that narrow features were in fact observed much earlier by RCPs in C-Mod IWL discharges [20]. The C-Mod IW is even more toroidally symmetric than on DIII-D, suggesting that it might in fact be local limiter misalignment which drives some of the strength in the narrow feature. New experiments have recently been performed including now IR imaging of the IW, but the data are unavailable at the time of writing.

Some evidence of double exponential feature in the SOL heat flux density profile in the IWL plasma has also recently been observed from the top RCP in the Tore Supra tokamak [31].

Figure 5 shows that the range of $\lambda_{q,near}^{OMP}$ is very similar in COMPASS, DIII-D, TCV and JET (though a somewhat smaller $\lambda_{q,near}^{OMP}$ is found in C-Mod), with the central value $\bar{\lambda}_{q,near}^{OMP} \approx 3$ mm. In addition, figure 6 illustrates clearly that the measured $\lambda_{q,near}^{OMP}$ vary strongly with $1/B_p^{OMP}$. Moreover, the narrow limiter widths are of the same magnitude, and follow

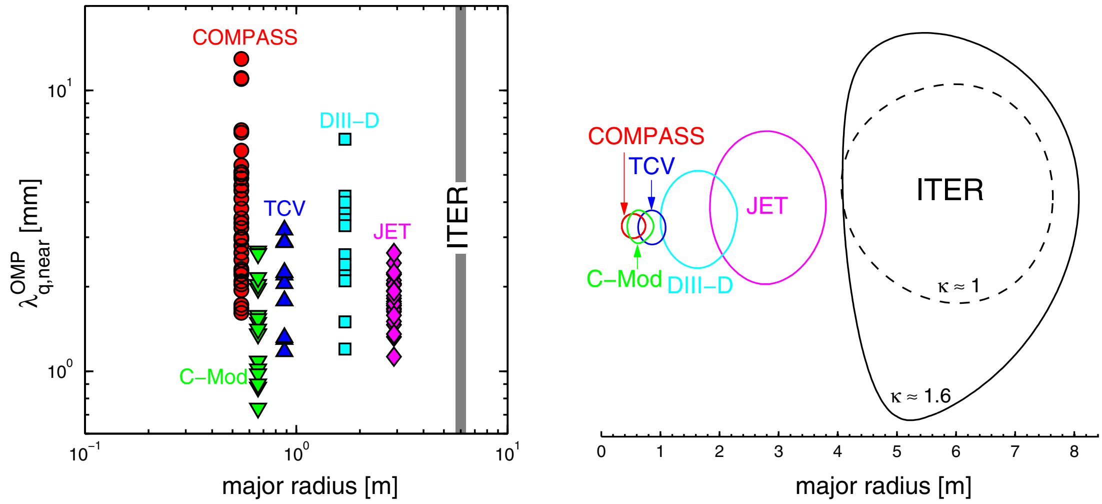

Figure 5. Left: $\lambda_{q,near}^{OMP}$ measured in different inboard-limited plasma experiments [10–14, 30], plotted as a function of R. Right: magnetic equilibrium reconstructions for typical discharges used for the experiments. Also shown for comparison are two representative ITER IWL start-up plasma equilibria.

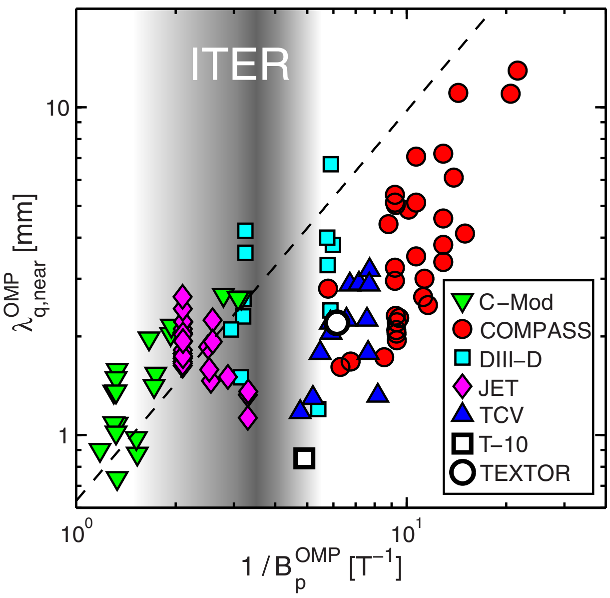

Figure 6. $\lambda_{q,near}^{OMP}$ measured in different inboard-limited plasma experiments [10–15, 18, 30], plotted as a function of $1/B_p^{OMP}$. Dashed: H-mode divertor plasma scaling from [32]. Shaded: approximate range of $1/B_p^{OMP}$ during IW start-up in ITER.

the same $1/B_p^{OMP}$ scaling as λ_q^{OMP} measured in H-mode divertor plasmas [32]. As shown in table 1 and as discussed in [33], the limiter narrow widths are also in reasonable agreement with the predictions of a 'heuristic drift-based' (HD) model [34]. The new $\lambda_{q,near}^{OMP}$ limiter data are well centred on the best-fit line of ~0.8 of the HD model prediction for the earlier H-mode divertor λ_q^{OMP} data (figure 1 in [33]) with scatter around this fit by a factor ~1.5 (figure 4 in [33]). This implies that $\lambda_{q,near}^{OMP}$ (limiter) $\approx\lambda_q^{OMP}$ (divertor) $\approx 1.6(a/R)\rho_{p,i}$, with $\rho_{p,i}$ the ion poloidal gyro-radius. The possible reasons for this similarity are discussed in [33]. Earlier work on limiter plasma [35] also predicted a SOL width of the order of $\rho_{p,i}$.

Alternative mechanisms which may drive a steepening of the near-SOL $q_\parallel$ have also been examined. As discussed

Table 1. Approximate range of $\lambda_{q,near}^{OMP}$ and R_q measured in different IWL experiments on five tokamaks [10–14, 30]. Also stated is the range of the near SOL e-folding length estimated from the HD model [33].

Tokamak	R_q	$\lambda_{q,near}^{OMP}$ (mm)	$\lambda_{q,near,HD}^{OMP}$ (mm)
C-Mod	2–4	1–3	1–3
COMPASS	2–5	2–8	2–10
DIII-D	~1	2–5	1–7
JET	1–6	2–4	2–4
TCV	2–4	1–3	1–3

in [11], non-ambipolar currents near the limiter apex can contribute up to ~45% to the observed steepening $q_\parallel$ in the near SOL, but are in general much lower and probably do not play a strong role. A further possibility is the effect of radial gradients of temperature and density induced by the limiter sink action. This speculation is consistent with EMC3-Eirene simulations of the originally planned ITER discrete OW limiters [36], which yield somewhat steeper $q_\parallel$ just outside the LCFS than further out in the main SOL, even though there is no double exponential $q_\parallel$ imposed in the simulations. In support of this effort to understand the narrow feature physics, EMC3-Eirene has been applied to the manufactured case of an IWL plasma in Tore Supra, including an artificial, toroidally discrete IW roof limiter. The results do not corroborate the hypothesis of an effect of the limiter sink in steepening the near-SOL heat flux profile [37].

Assuming then that an ion poloidal gyro-radius scaling is a reasonable physics basis for extrapolation to ITER and given the scatter in the currently available experimental data (figures 5 and 6), a characteristic value of $\lambda_{q,near}^{design} = \bar{\lambda}_{q,near}^{OMP} f_x =$ 4 mm can be adopted for the ITER IW FWP toroidal shape. Here, $f_x \approx 1.3$ is the poloidal flux expansion factor between the IW and the OMP for ITER IW limiter configurations. As will be discussed in section 6.1, the sensitivity of new IW FWP toroidal profile proposed here to power handling is weaker than this experimental data scatter for $\lambda_{q,near}^{design}$ in the range 2–8 mm.

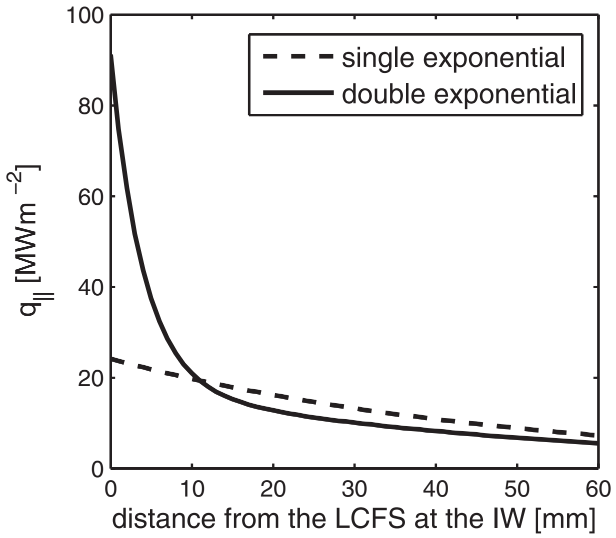

Figure 7. Radial profiles of $q_{\|}$ obtained from equation (1) for $\lambda_{q,main}^{design} = 50$ mm and $R_q = 0$ (single exponential) and $\lambda_{q,main}^{design} = 50$ mm, $\lambda_{q,near}^{design} = 4$ mm and $R_q^{design} = 4$ (double exponential). $P_{SOL} = 5$ MW in both cases.

Turning now to the value of parameter R_q, the measured value (table 1) falls within the range ~1–6. With the exception of C-Mod, which is not currently understood, the lowest R_q values are observed for a toroidally nearly symmetric IW. The tendency for R_q to increase with the limiter radial misalignment, Δ_r can be related to the way in which IW limiters share the incident double exponential $q_{\|}$. A limiter misaligned by $\Delta_r \approx \lambda_{q,near}$ intercepts a larger fraction of $q_{\|,near}$, whilst $q_{\|,main}$ remains almost equally distributed between all IW limiters (since $\Delta_r \approx \lambda_{q,near} \ll \lambda_{q,main}$), making the effective R_q for the radially misaligned limiter larger. This argument (supported partially by the measurements (table 1), suggests that in case of perfectly aligned IW limiters in ITER, it would be reasonable to expect $R_q \approx 1$ for IWL plasmas. However, since assembly errors are inevitable for the ITER Blanket system [3], it seems more appropriate to adopt a larger value of R_q. Inspection of the scatter in this parameter in table 1 indicates that $R_q^{design} = 4$ is a reasonable choice for ITER. As will be shown later, the new toroidal shape proposed for ITER to account for the narrow feature has some margin for variation in R_q and thus the choice of a roughly median value from the data available today seems acceptable.

The radial profile of $q_{\|}$ evaluated for $\lambda_{q,main}^{design} = 50$ mm, $\lambda_{q,near}^{design} = 4$ mm, $R_q^{design} = 4$ is compared in figure 7 with the single exponential profile obtained for $\lambda_{q,main}^{design} = 50$ mm. In both cases, $P_{SOL} = 5$ MW has been assumed. Note that since $\lambda_{q,near}^{design} \ll \lambda_{q,main}^{design}$, the double exponential $q_{\|}$ profile is up to a factor ~4 larger in the near SOL, but only about 25% lower in the main SOL compared to the single exponential $q_{\|}$ case.

As was already mentioned, enhanced heat fluxes near limiter tangency points is not a new feature and has been observed much earlier on tokamaks [15–19], though these early clues were not more thoroughly investigated. As a consequence, there was insufficient physics understanding to account for the effect in the original ITER IW FWP design. Furthermore, there are good reasons to believe that in some of these earlier experiments the enhanced heat loads near the limiter apexes are due not to a narrow near-SOL $q_{\|}$ feature, but instead to a cross-field heat flux, $q_{cross\text{-}field}$, to the limiter, itself enhanced by the presence of the limiter. This perpendicular transport is believed to occur only at vanishing field line incidence angles, $\alpha_{inc} < (m_e/m_i)^{1/2} \approx 1°$ for a deuterium plasma (as was assumed in [38, 39] based on earlier work by Chodura [40] and Holland [41]), which is significantly less that α_{inc} at the apex of the original IW FWPs and still somewhat less than α_{inc} for the new IW FWP shape proposed in this paper (section 6.1). It is important to note that even if this $q_{cross\text{-}field}$ did occur in ITER, its effect would be only to increase (and not decrease) the plasma wetted area by depositing heat flux on the surfaces which are magnetically shadowed. This would reduce peak heat fluxes and it is thus in fact conservative to neglect $q_{cross\text{-}field}$ in the FWP shaping analysis.

Returning to the RCP measurements from the more recent experiments, the inconsistent evidence for a double-exponential $q_{\|}$ in the probe data can be associated with a number of factors. The probe spatial resolution (determined by the radial dimension of a probe collector and the voltage sweep frequency relative to the stroke speed when the single-probe technique is used) is typically a few mm, so that the narrow feature can be smeared out on the measured $q_{\|}$ profile. Additionally, most RCP systems tend to be configured for reciprocation into the SOL plasma poloidally quite far from the IW, making measurements of the narrow near-SOL feature even more difficult due to the flux compression. Probe measurements of $q_{\|}$ in the near-SOL might (among other uncertainties) [42] be flawed by a perturbation of the local plasma (and hence a perturbation of n_e and T_e) as a result of impurity release or fuel recycling from the probe itself [27]. The influence of these factors depends on the probe design and operation as well as on the plasma and the location being probed, which might explain why some RCP measurements clearly show the narrow near-SOL feature and others do not.

5. New IW FWP toroidal shape profile

Armed with proposed values for $\lambda_{q,near}^{design}$, $\lambda_{q,main}^{design}$ and R_q^{design}, a new toroidal shape profile for the ITER IW FWPs, $f(t)$, can be constructed which would optimize the distribution of q_{surf} in the presence of a double exponential SOL heat flux profile. The analysis is based on the analytical expressions developed in [23] for the ITER OW FWP shaping.

Defining

$$q_{||0,ref} = \frac{P_{SOL}}{4\pi R_{IW} \lambda_{q,ref} \left(\frac{B_p}{B_{total}}\right)_{IW}} \tag{4}$$

and

$$q_{||0,near,main} = \frac{P_{near,\,main}}{4\pi R_{IW} \lambda_{q,near,main} \left(\frac{B_p}{B_{total}}\right)_{IW}}, \tag{5}$$

where $P_{SOL} = P_{near} + P_{main}$, leads to

$$\frac{q_{||0,main}}{q_{||0,ref}} = \left[\left(\frac{\lambda_{q,main}}{\lambda_{q,ref}}\right) + R_q \left(\frac{\lambda_{q,near}}{\lambda_{q,ref}}\right)\right]^{-1} \equiv R_{q,main} \tag{6}$$

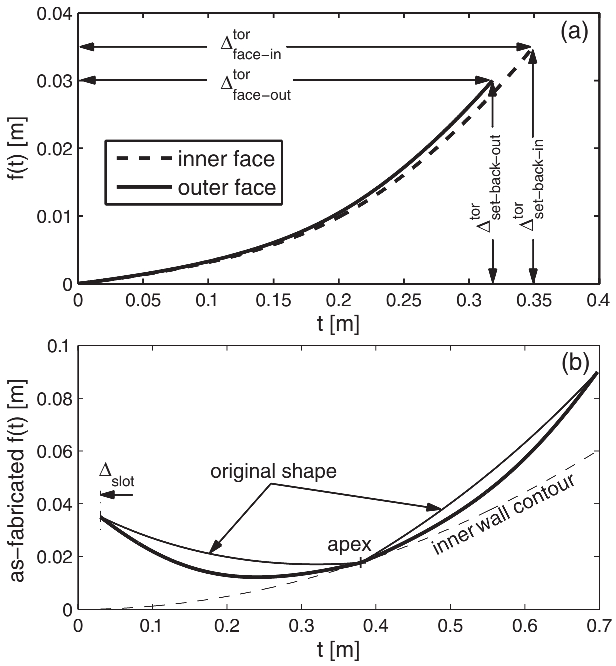

Figure 8. (*a*) Toroidal profile of the inner and the outer face of the new ITER IW limiter optimized for double exponential $q_\parallel$ with $\lambda^{design}_{q,main} = 50$ mm, $\lambda^{design}_{q,near} = 4$ mm, $R^{design}_{q} = 4$. (*b*) 'As-fabricated' toroidal profile. Also shown for comparison is the original FWP toroidal shape. Vertical axis is greatly exaggerated for clarity.

and

$$\frac{q_{||0,near}}{q_{||0,ref}} = R_q R_{q,main} \equiv R_{q,near}. \tag{7}$$

Thus, the normalized deposited power flux density just due to the toroidal component of $q_\parallel$ is given approximately by

$$\hat{q}^{tor}_{surf}(t) \equiv \frac{q^{tor}_{surf}}{q_{||0,ref}} = f'\left[\left(\frac{q_{||0,main}}{q_{||0,ref}}\right)e^{-f(t)/\lambda_{q,main}} + \left(\frac{q_{||0,near}}{q_{||0,ref}}\right)e^{-f(t)/\lambda_{q,near}}\right] = f'\left[R_{q,main}e^{-f(t)/\lambda_{q,main}} + R_{q,near}e^{-f(t)/\lambda_{q,near}}\right], \tag{8}$$

where $f' = \mathrm{d}f/\mathrm{d}t$ with $f(t)$ the required toroidal shape function and the location $t = 0$ defined at the limiter leading point (apex). Additionally, $\lambda_{q,ref} = \lambda_{q,main}$ has been assumed in equation (8). Since the peak power deposition is strongly dominated by the toroidal component of $q_\parallel$, the toroidal shaping is nearly optimized by requiring that $\hat{q}^{tor}_{surf}(t) = C$, with C a constant to be found [23]. This results in a nearly uniform power loading of the surface, tending to minimize q_{peak}. Integrating equation (8) gives:

$$R_{q,main}\lambda_{q,main}\left(1 - e^{-f(t)/\lambda_{q,main}}\right) + R_{q,near}\lambda_{q,near}\left(1 - e^{-f(t)/\lambda_{q,near}}\right) = Ct \tag{9}$$

from which the value of C can then be found by requiring that $f(t) = \Delta^{tor}_{set-back}$, the toroidal limiter 'set-back' at the ends of the profile [23], figure 8(*a*). This can only be solved numerically except if $R_q = 0$, in which case the original logarithmic IW FWP toroidal profile is obtained. Several additional 'anchor points' shown in figure 8(*a*) are also required to specify the profile: the FWP toroidal spans ($\Delta^{tor}_{face-in} = 0.3495$ m and $\Delta^{tor}_{face-out} = 0.318$ m for the 'standard' IW FWPs, ignoring FWP variants with the diagnostic cut-outs); toroidal set-backs ($\Delta^{tor}_{set-back-in} = 0.035$ m and $\Delta^{tor}_{set-back-out} = 0.03$ m, required for protecting the FWP toroidal edges); and the IW radius ($R_{IW} = 4.08$ m). The anchor points used for the original IW FWP logarithmic toroidal profile are retained for the new shape. The asymmetry between $\Delta^{tor}_{face-in}$ and $\Delta^{tor}_{face-out}$ requires C to be evaluated separately for the inner and the outer face:

$$R_{q,main}\lambda_{q,main}\left(1 - e^{-\Delta^{tor}_{set-back-out}/\lambda_{q,main}}\right) + R_{q,near}\lambda_{q,near} \times \left(1 - e^{-\Delta^{tor}_{set-back-out}/\lambda_{q,near}}\right) = C_{outer}\Delta^{tor}_{face-out} \tag{10}$$

and

$$R_{q,main}\lambda_{q,main}\left(1 - e^{-\Delta^{tor}_{set-back-in}/\lambda_{q,main}}\right) + R_{q,near}\lambda_{q,near} \times \left(1 - e^{-\Delta^{tor}_{set-back-in}/\lambda_{q,near}}\right) = C_{inner}\Delta^{tor}_{face-in}. \tag{11}$$

For the case of $R_q = R^{design}_q = 4$, $\lambda_{q,near} = \lambda^{design}_{q,near} = 4$ mm and $\lambda_{q,main} = \lambda^{design}_{q,main} = 50$ mm, equations (10) and (11) yield $C_{outer} = 0.0918$ and $C_{inner} = 0.0892$. Note that $\Delta^{tor}_{face-out} < \Delta^{tor}_{face-in}$ is compensated by $\Delta^{tor}_{set-back-out} < \Delta^{tor}_{set-back-in}$, resulting in $C_{outer} \approx C_{inner}$, i.e. almost the same q_{peak} for the inner and the outer face. The choice of the set-back values is determined by the dual (and conflicting) criteria that toroidal edges must be hidden from plasma impact at the same time as maximizing the plasma wetted area [23].

Figure 8(*a*) illustrates the inner and the outer face toroidal profiles optimized for power handling in the presence of the narrow heat flux feature, obtained from equations (10) and (11). These profiles actually represent the distance from the LCFS to the limiter surface. In figure 8(*b*), these profiles are converted into an 'as-fabricated' IW FWP toroidal shape by taking into account the IW curvature. Figure 9 illustrates the rather small differences between the original logarithmic FWP toroidal profile and the new variant optimized for the double exponential heat flux profile.

There are two implications of using the same anchor points for the original and the new limiter toroidal profile: (i) the shape change requires that material be added (up to ~7 mm in places) to accommodate the enhanced $q_\parallel$ near the apex, and (ii) smaller α_{inc} near the apex for the new shape leads to larger α_{inc} near the central slot and the toroidal edge, making these areas potentially prone to larger q_{peak} if exposed to the plasma.

6. IW FWP surface heat loads

Since, as explained in section 4, the physics basis for the choice of key shaping parameters ($\lambda^{design}_{q,near}$, $\lambda^{design}_{q,main}$ and R^{design}_q) for a modified IW toroidal profile is expected to be subject to further refinement, it is important to study the power handling sensitivity of the new shape to reasonable variations in both $q_\parallel$ and the shape parameters themselves. In particular, this section asks: (i) what would be the heat load if the IW FWP shape is not modified and the narrow heat flux feature does turn out to be present in ITER limiter plasmas (to which all current evidence points); and (ii) what would be the heat load if the new IW FWP shape is adopted and the narrow feature turned out to be absent in ITER? These questions are studied here by simulating surface heat loads on the IW FWPs for ITER start-up equilibria,

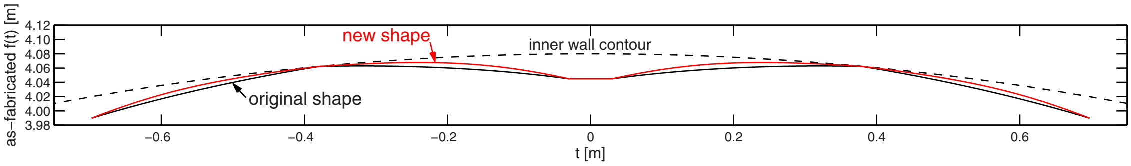

Figure 9. Toroidal profile of the original and the new IW FWPs in ITER, optimized for the $q_{\parallel}$ profiles in figure 7.

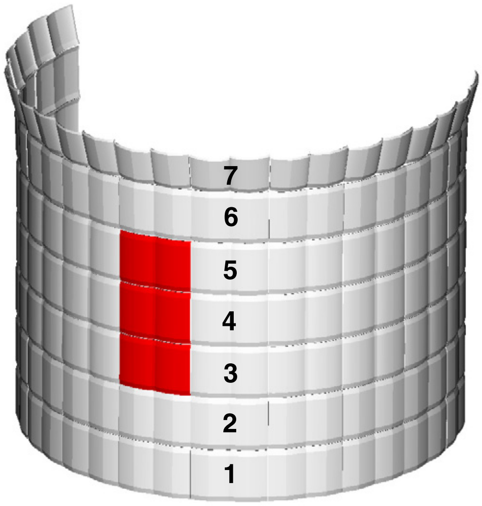

Figure 10. Model of the ITER IW used for the field line tracing calculations. The three FWPs studied are highlighted. Numbers indicate FWP poloidal rows.

using magnetic field line tracing taking into account the full, three-dimensional structure of the FWPs, including magnetic shadowing effects.

Figure 10 illustrates the model used to investigate the IW FWP surface heat load, which assumes an axisymmetric plasma and considers FWPs 3–5 only at a single toroidal location. The remaining panels in the model, which include five toroidal neighbour panels and the poloidal rows 1–2 and 6–7, act as magnetically shadowing objects. The FWPs are represented by triangular surface grids with 2–5 mm spatial resolution (higher on the poloidal edges and lower on the limiter face). Details of the FWP design such as surface castellation, faceting and the central slot are omitted in the model.

The modified toroidal shape is applied to FWPs 3–5, with the remaining rows retaining the original logarithmic profile optimized for a single exponential SOL heat flux profile. Choosing to restrict the modification to only the three central panels has important engineering implications in view of the late hour at which the change is being introduced. By leaving rows 1–2 and 6–7 unchanged, considerable savings are made in the efforts required to re-engineer the FWP. In addition, since the limiter function for start-up is restricted only to FWP 3–5, there is no *a priori* need to modify panels other than those in the midplane region. However, this approach introduces transition in the toroidal shape between FWPs 2–3 and 5–6, an issue which is addressed in section 6.2. The FWP poloidal profile consists of a straight face with a chamfer (to protect poloidal edges) [23] starting 0.1 m from the poloidal edge, where it reaches the recess value $\Delta^{pol}_{set\text{-}back} = 0.03$ m.

A rather conservative approach is adopted here in testing the new FWP shape by assuming that the investigated FWP is radially advanced by a distance $\Delta_r = 5$ mm with respect to all the other FWPs (assumed perfectly aligned). This corresponds to the estimated FWP radial alignment tolerance. The objective is to investigate if, in the absence of the narrow heat flux feature, the radial misalignment could lead to large q_{peak} on the new panel shape, for which α_{inc} is larger further away from the apex compared with the original FWP toroidal shape.

The plasma wetted area is obtained from the field line tracing code PFCFLUX [43]. Magnetic field lines emanating from each grid node on the FWP surface contour are tracked for up to $L_{max} = 8$ m. The node is flagged as magnetically shadowed if intersection occurs on any IW surface within L_{max}. Field lines which leave the area without intersecting any limiter surface are assumed to result in exposure to the SOL plasma of the corresponding location on the FWP. Artificial ridges are placed at the rear of the panels to eliminate unphysical wetted areas due to field lines striking from behind the panels through gaps between panels. The number of target panel toroidal neighbours and L_{max} are made large enough to obtain a complete shadow pattern, given that for most IWL plasma equilibria the magnetic shadow is not entirely due to the nearest neighbour FWP. This is particularly important when q_{peak} occurs near or at the shadow line. For each of the plasma-wetted nodes, q_{surf} is evaluated as $q_{\parallel}\sin(\alpha_{inc})$ with $q_{\parallel}$ profiles from figure 7. Radiative heat load (due to charge exchange neutrals and photons) is assumed to be zero during plasma start-up, as are add-on penalties due to assembly errors (other than Δ_r) and panel faceting (see section 3 and [29]).

6.1. Heat load on the IW FWP face

Figure 11 gives the poloidal distribution of q_{surf} on FWP 4 for an ITER IW start-up plasma corresponding approximately to the largest anticipated I_p (∼5 MA) before X-point formation in the currently available scenario designs (see figure 1). The magnetic equilibrium reconstruction is also given in the figure for reference. This plasma has $B_t = 5.3$ T, elongation $\kappa = 1.6$, $q_{LCFS} = 10$ and $P_{SOL} \approx I_p = 5$ MW is assumed.

The surface heat load is calculated for different combinations of $q_{\parallel}$ profiles from figure 7 and the FWP toroidal profiles from figure 9. Figures 11(*a*),(*d*) and (*b*),(*c*) thus correspond, respectively, to the optimal and non-optimal combinations of the limiter toroidal profile and $q_{\parallel}$. For the original logarithmic profile exposed to a single exponential heat flux profile, $q_{peak} \approx 2$ MW m^{-2} and is located on the poloidal chamfer. For the new toroidal shape, the heat load peaks toroidally further away from the apex (where α_{inc} is larger, figure 12) reaching $q_{peak} \approx 2.2$ MW m^{-2}, about 10% larger than for the original logarithmic profile. In the presence of the narrow heat flux channel, $q_{peak} \approx 5.5$ MW m^{-2}

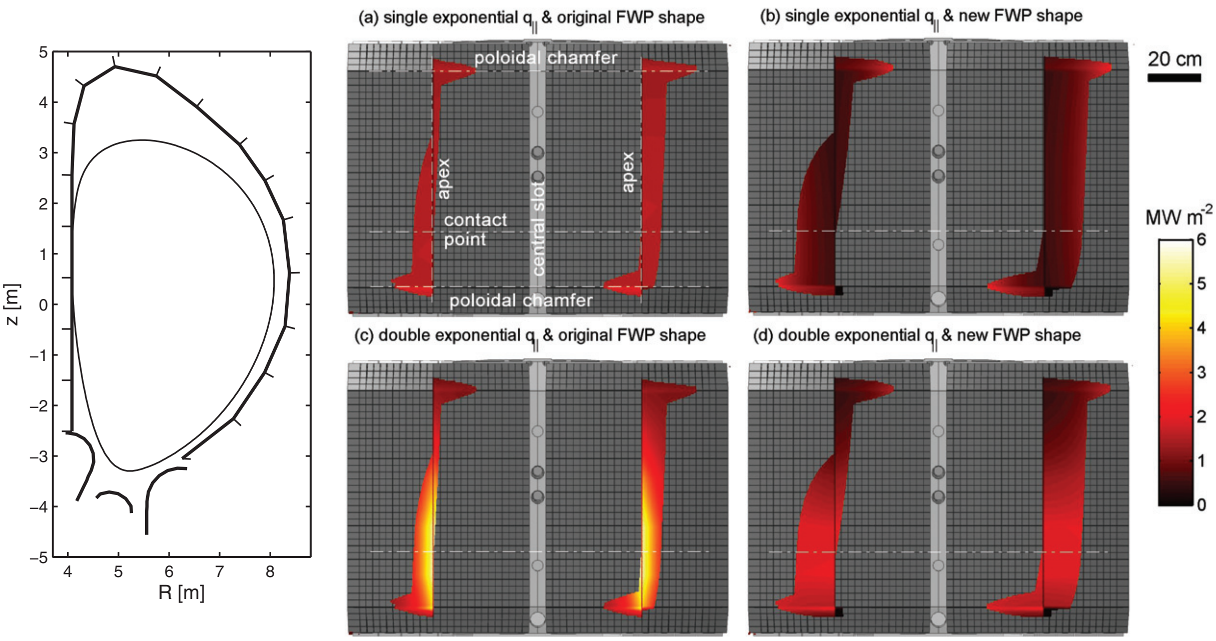

Figure 11. Surface heat load on the plasma-wetted area of FWP 4, evaluated for single (a, b) and double exponential (c, d) $q_{\|}$ from figure 7 for the original (a, c) and the new FWP toroidal profile (b, d) from figure 9, assuming $\Delta_r = 5$ mm. IWL plasma with $P_{\rm SOL} \approx I_{\rm p} = 5$ MW/MA. The magnetic equilibrium reconstruction is also shown.

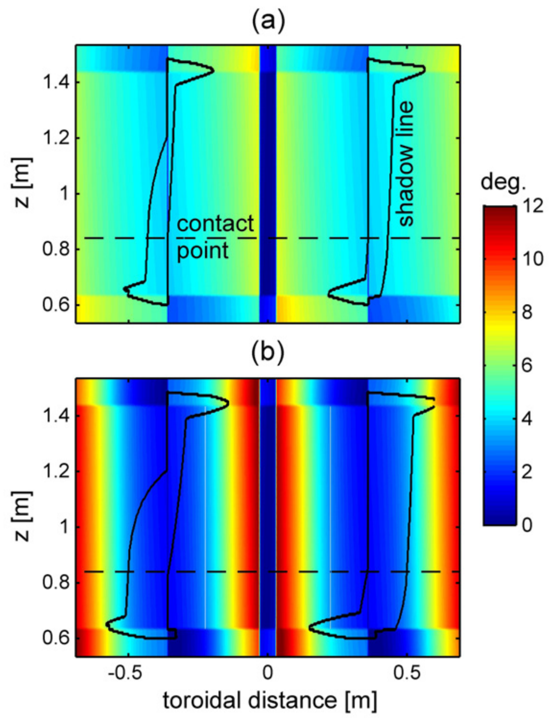

Figure 12. Field line incidence angle on FWP 4 featuring (a) original and (b) new toroidal profile. Also shown is the magnetic shadow line calculated assuming $\Delta_r = 5$ mm. Corresponding plasma equilibrium is shown in figure 11.

(considerably larger than $q_{\rm peak}^{\rm design}$, even without additional penalty factors) is found just at the apex of the logarithmic shape due to the enhanced $q_{\|}$ in the near-SOL. In contrast, and as expected, the double exponential $q_{\|}$ profile results in a much more uniformly distributed heat flux, with a much lower $q_{\rm peak} \approx 2.2$ MW m^{-2} (coincidentally very similar to the value obtained for the single exponential heat flux profile, but in a different location). For this plasma equilibrium the heat loads on FWP 3 and 5 are lower than on FWP 4 due to larger $\Delta r_{\rm LCFS}$ and are not shown.

Figure 11 thus illustrates that without the toroidal profile modification, the original IW FWPs would have a much larger heat load if the narrow feature does occur in ITER limiter plasmas. On the other hand, for the $\Delta_r = 5$ mm assumed here, the new limiter shape reduces the power handling by only ~10% if the narrow heat flux feature does not occur. If $\Delta_r < 3$ mm were instead assumed, $q_{\rm peak}$ in the absence of the narrow feature would be the same for both limiter toroidal profiles shapes. As discussed in section 4 and [12], however, the combination of strong misalignment and a single exponential $q_{\|}$ profile would seem unlikely, since measurements show that the intensity of the narrow feature is enhanced ($R_{\rm q}$ increases) when a given limiter is protruding into the plasma by a few mm. Given the estimated 5 mm maximum panel-to-panel radial alignment tolerance in ITER, it is very likely that some FWPs will indeed protrude to distances ~$\lambda_{\rm q,near}$, leading to large $R_{\rm q}$. This effect is actually anticipated in the choice of a relatively large $R_{\rm q}^{\rm design} = 4$ for the new IW FWP toroidal profile. This also means that without the toroidal profile modification, the original logarithmic IW FWPs would need even tighter assembly tolerances to mitigate the intensity of the narrow feature should it occur. Achieving such assembly tolerances would be extremely challenging.

Note that the wetted area of the original limiter geometry shown in figure 11 is smaller than for the new limiter shape. At first sight, this may be taken to suggest that the original limiter shape was not really optimized even for the assumption of a single exponential $q_{\|}$, because the heat load is concentrated on

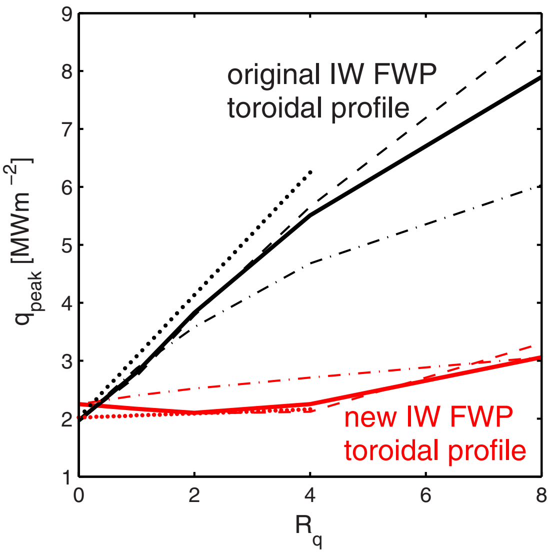

Figure 13. Peak surface heat load on FWP 4 with the toroidal profiles from figure 9, optimized for $q_\parallel$ with and without the narrow feature, plotted as a function of R_q ($\Delta_r = 5$ mm, $P_{SOL} = I_p = 5$ MW/MA, $B_t = 5.3$ T). Simulations are performed for $\lambda_{q,near} = 2$ (dashed) 4 (full) and 8 mm (dashed–dotted) with $\lambda_{q,main} = 50$ mm. Dotted: analytic calculation.

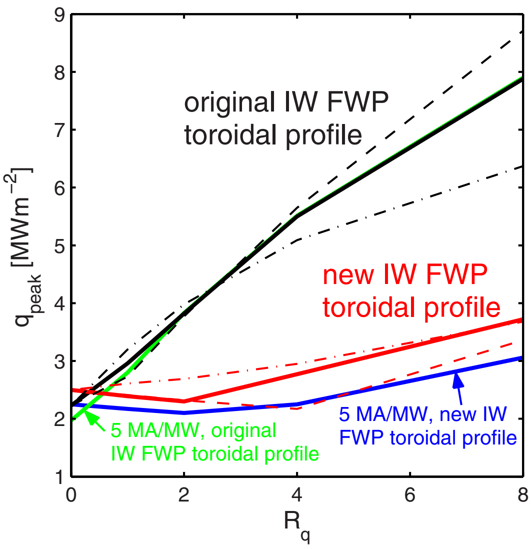

Figure 14. Peak surface heat load on FWP 4 obtained for the same plasma equilibrium and $q_\parallel$ profiles as in figure 13 but with $I_p = 7.5$ MA ($P_{SOL} = 7.5$ MW). Simulations are performed for $\lambda_{q,near} = 2$ (dashed) 4 (full) and 8 mm (dashed–dotted) with $\lambda_{q,main} = 50$ mm. Also shown for comparison is q_{peak} obtained for $I_p = 5$ MA ($P_{SOL} = 5$ MW), repeated from figure 13, assuming $\lambda_{q,near} = 4$ mm.

a too small fraction of the limiter surface. However, as stated in section 5 and in [23], the aim of toroidal shape optimization is to achieve the smallest possible q_{peak}, for a specified $q_\parallel$ profile, while protecting the FWP edges. While there is a tendency for that to correspond to maximizing wetted area, it is not the same thing since most of the wetted area involves q_{surf} values less than the value of q_{peak} [23] so whether the wetted area is large or small is not the critical issue.

The effect on q_{peak} (the maximum of q_{surf}, wherever it occurs on the surface) of varying the strength of the narrow feature (variation of R_q) is illustrated in figure 13 for the original and new toroidal shapes, again considering the central FWP 4. Focusing first on the limiter shape optimized for power handling in the presence of the narrow feature, q_{peak} is approximately constant for $R_q = 0$–5. This range encompasses most of the measured R_q values. For $R_q < 8$, $q_{peak} < 3$ MW m^{-2}, well below q_{peak}^{design}. At the same time, q_{peak} is only weakly sensitive to $\lambda_{q,near}$. Note that the curves in figure 13 obtained for $\lambda_{q,near} = 2$ and 8 mm (100% variation around $\lambda_{q,near}^{design}$) do not represent a confidence interval around $\lambda_{q,near} = 4$ mm, but merely reflect the variation of q_{peak} with $\lambda_{q,near}$ due to the complex FWP shape. For example, at $R_q = 7$, $\lambda_{q,near} = 2$ and 8 mm both lead to the same q_{peak} (albeit on different wetted area locations), and in both cases the value is slightly larger than that obtained for $\lambda_{q,near} = 4$ mm.

In the case of the original logarithmic limiter shape, q_{peak} is similar (10% lower) to that obtained for the new shape in the absence of the narrow feature, but increases strongly with R_q due to enhanced power deposition the apex. For $R_q > 3$, q_{peak} exceeds q_{peak}^{design} even without add-on penalties and irrespective of the value of $\lambda_{q,near}$. The same heat load calculation, but assuming a single exponential $q_\parallel$ with $\lambda_{q,main} = 25 \rightarrow 100$ mm at the IW (50% variation around $\lambda_{q,main}^{design}$), yields a very similar range of $q_{peak} = 3.6 \rightarrow 1.1$ MW m^2 and $q_{peak} = 3.4 \rightarrow 1.4$ MW m^2 for the logarithmic and the new limiter shapes, respectively. Also included in figure 13 is an estimate of q_{peak} from the analytic model developed in [23]. The analytic model agrees within ~10% on average with the numerical calculation, corroborating the field line tracing results.

Even though the present study concentrates on $I_p = 5$ MA (corresponding to the largest anticipated plasma current before X-point formation in the currently available scenario designs), as highlighted in section 2, the ITER Heat Load Specifications actually prescribe that the IW and OW FWPs must tolerate steady state limiter operation at $I_p \leqslant 7.5$ MA. The rationale of this requirement is to provide some margin with respect to the expectations of scenario design and to provide for flexibility in the earlier phases of ITER operation.

In order to test the power handling properties of the new as well as the original IW FWP toroidal profiles at this maximum required I_p, the heat load calculation from figure 13 has been reproduced for the same plasma equilibrium as in figure 11 but with I_p increased to 7.5 MA. The result is shown in figure 14, which has been obtained by rescaling the pitch angle to give the equivalent field line angle geometry for the 7.5 MA/5.3 T and assuming, as before $P_{SOL} = I_p$ and $\Delta_r = 5$ mm. The increase of I_p from 5 to 7.5 MA does not change the conclusions regarding the need for the new IW FWP shape. The only difference is a slightly higher q_{peak} due to somewhat steeper incidence angle for the increased current. Note that for $R_q = 0$–1 the increase of q_{peak} is the same for both FWP shapes. In addition, the same heat load calculation, but assuming a single exponential $q_\parallel$ with $\lambda_{q,main} = 25 \rightarrow 100$ mm at the IW, yields a very similar range ($q_{peak} = 4.1 \rightarrow 1.2$ MW m^2) for the original and for the new ($q_{peak} = 3.7 \rightarrow 1.6$ MW m^2) limiter shapes at 7.5 MA.

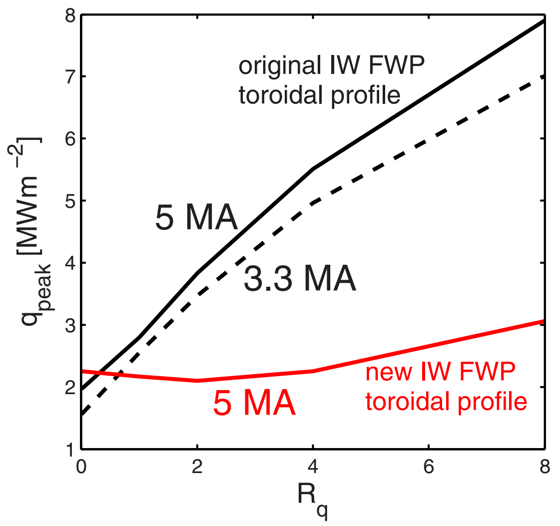

Figure 15. Comparison of q_{peak} on FWP 4 from figure 13 (for $P_{\text{SOL}} = 5$ MW and $I_p = 5$ MA) with q_{peak} calculated for the original FWP logarithmic toroidal profile assuming $P_{\text{SOL}} = I_p = 3.3$ MW/MA and otherwise identical parameters ($\lambda_{q,\text{main}} = 50$ mm, $\lambda_{q,\text{near}} = 4$ mm, $B_t = 5.3$ T, $\kappa = 1.6$, $\Delta_r = 5$ mm).

Regarding the effect of plasma elongation on the IW FWP surface heat load, a somewhat larger q_{peak} for both limiter shapes is generally obtained from the field line tracing for a circular plasma for the same I_p and P_{SOL}. This increase in q_{peak} with the decreasing κ is due to larger LCFS curvature (thus larger α_{inc}) near the plasma contact point and is somewhat larger for the original logarithmic FWP toroidal shape.

In addition to the radial misalignment, a further potential FWP assembly error is a tilt along the panel vertical axis (α_{tilt} up to 0.2°), which increases the toroidal component of α_{inc} and leads to larger q_{peak} (since q_{surf} is determined mainly by the toroidal component of $q_{||}$). However, field line tracing simulations identical to those in figure 13 but with $\alpha_{\text{tilt}} = 0.2°$, find only small differences in q_{peak}. This is due to the fact that for both the original and new IW FWP toroidal shapes, $\alpha_{\text{inc}} \gg \alpha_{\text{tilt}}$ at the location of q_{peak}, making q_{surf} in these locations relatively insensitive to a small tilt.

It could be argued that since $P_{\text{SOL}} = I_p = 5$ MW/MA assumed in the analysis of figure 13 is ~50% higher than the minimum current at which the X-point can be formed in present scenario designs, q_{peak} may be acceptable at these lower currents for the original limiter, even in the presence of the narrow heat flux feature. In order to test this hypothesis, q_{surf} is evaluated for the original IW FWP shape assuming the ITER start-up plasma equilibrium characterized by $I_p \approx$ 3.3 MA (assuming again $P_{\text{SOL}} = I_p$) which represents, approximately, the minimum required I_p value at X-point formation (section 2). In this case, somewhat larger e-folding lengths are assumed due to the lower I_p : $\lambda_{q,\text{main}} = 60$ mm and $\lambda_{q,\text{near}} = 5$ mm at the IW, estimated respectively from the new scaling for $\lambda_{q,\text{main}}$ [24] and assuming the HD/poloidal gyro-radius scaling [33, 34]. As shown in figure 15, q_{peak} is reduced only by ~0.5 MW m^{-2} for $I_p = 3.3$ MA compared with $I_p = 5$ MA for the logarithmic shape and the single exponential heat flux profile. This is due to the fact that for fixed λ_q, $q_{\|,0} \propto P_{\text{SOL}}/(B_p/B_t)$ from power balance (equation (2)) is independent of I_p if I_p is assumed to be of the same magnitude as P_{SOL}, as required by the ITER Heat Load Specifications. The slightly lower q_{peak} at $I_p = 3.3$ MA is thus due mainly to the increased $\lambda_{q,\text{main}}$ at lower I_p assumed here. Figure 15 shows clearly that the limiter optimized for power handling in the presence of the narrow feature actually performs much better at 5 MW/MA than the original limiter at 3.3 MW/MA in the presence of the enhanced near-SOL heat flux.

It is interesting that q_{peak} on the original logarithmic FWP shape is much higher in the presence of the narrow feature than in the case of a single exponential heat flux profile, but is only slightly higher on the new limiter shape in the absence of the narrow feature, even for large Δ_r. The striking difference in the power handling performance of these two FWP toroidal shapes can be explained by magnetic shadowing which masks the areas of the FWP toroidally further away from the apex where α_{inc} is larger for the new FWP shape (figure 12) and where q_{peak} would have occurred in the absence of the narrow feature. This beneficial shadow-masking was already pointed out in [23] for the general case of $\lambda_q > \lambda_q^{\text{design}}$, which is analogous to new FWP shape exposed to the plasma without the narrow feature. On the other hand, magnetic shadowing does not prevent elevated q_{peak} on the original logarithmically shaped FWP, for which the peak region of q_{surf} in the presence of the narrow feature occurs right at the apex.

In general, this shadow-masking becomes less effective when both the field line pitch and the LCFS curvature are large. This can potentially lead to exposure of the outer parts of the limiter face to the plasma and thus to high q_{peak} on the new FWP shape if the narrow feature did not occur on ITER. The largest LCFS curvature occurs for circular plasmas and the largest field line pitch when B_t is low and I_p high. The lowest B_t envisaged for ITER operation will be 2.65 T, half the nominal field, which will be most often used in the non-active operation years to allow more ready access to H-mode plasmas [44]. Diverted plasmas in this case will use $I_p = 7.5$ MA to provide the same edge safety factor as for baseline 15 MA/5.3 T operation, but for circular IWL plasmas the maximum current will be limited to much lower values for stability reasons. However, to be conservative, a circular 5 MA plasma case at 2.65 T has been examined, taking the usual maximum radial misalignment of 5 mm. Figure 16 illustrates the power flux distribution on an inner midplane FWP 4 with the new toroidal shape for a single exponential $q_{\|}$ profile with varying $\lambda_{q,\text{main}} = 25$, 50 and 100 mm. As $q_{\|}$ broadens, the location of q_{peak} moves toroidally further away from the apex due to a higher $q_{\|}$ in the far-SOL. However, due to lower $q_{\|,0} \propto P_{\text{SOL}}/(B_p/B_t)$ at lower B_t, the highest $q_{\text{peak}} = 1.6$ MW m^{-2} (at $\lambda_{q,\text{main}} = 25$ mm) observed in this half-B_t plasma configuration is even lower than that observed for the full field plasma at the same P_{SOL}. The field line tracing runs for the new IW FWP shape assuming a single exponential $q_{\|}$ with $\lambda_{q,\text{main}} = 25 \rightarrow 100$ mm and the plasma equilibrium from figure 14 ($P_{\text{SOL}} = I_p = 7.5$ MW/MA) but with $B_t = 2.65$ T, yield $q_{\text{peak}} = 2.3 \rightarrow 0.9$ MW m^{-2}. This is almost a factor 2 lower than the $q_{\text{peak}} = 3.7 \rightarrow$ 1.6 MW m^{-2} obtained for the same plasma equilibrium and I_p, but assuming $B_t = 5.3$ T. This is due to the higher field line pitch angle at lower B_t and thus lower $q_{\|}$ (see equation (2)).

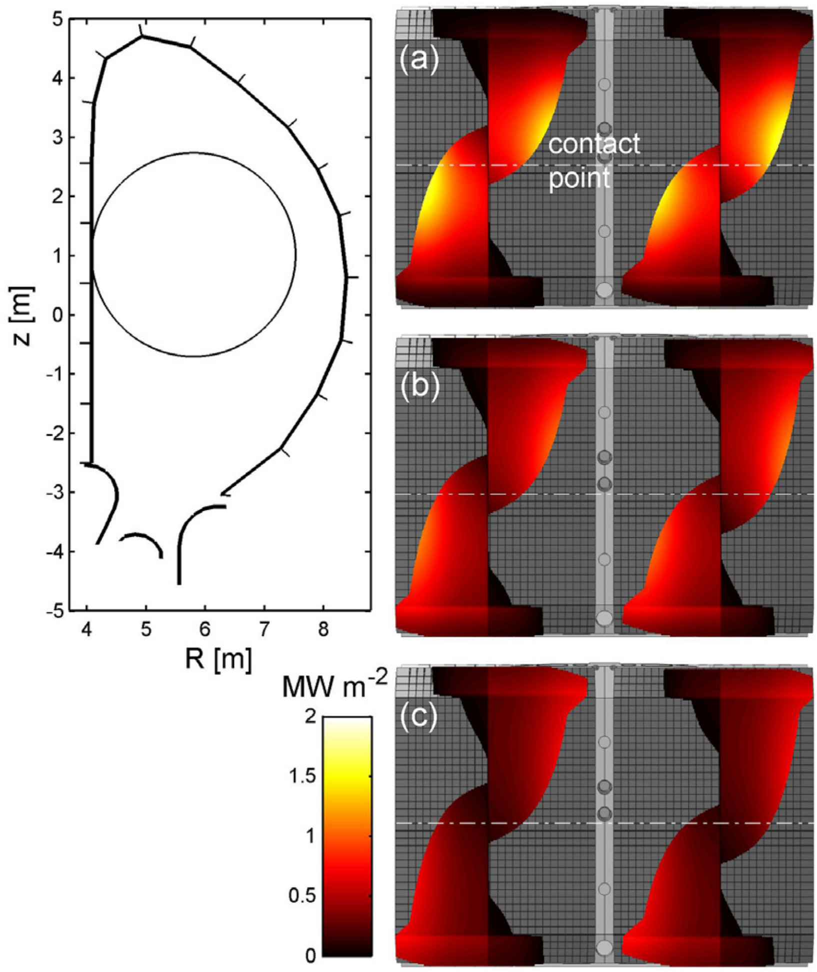

Figure 16. Surface heat load (without add-on penalty factors) on the plasma-wetted area of FWP 4 optimized for the power handling in the presence of the narrow feature. IWL plasma with $B_t = 2.5$ T, $P_{SOL} = I_p = 5$ MW/MA and a single exponential $q_{||}$ with (*a*) $\lambda_{q,main} = 25$ mm, (*b*) 50 mm and (*c*) 100 mm. As before, the target FWP is radially misaligned by 5 mm. The magnetic equilibrium reconstruction is also shown.

Before proceeding further, a comment is appropriate with regard to the FWP surface castellation, omitted in the field line tracing model. Since adjacent Be tiles on the toroidal fingers making up the FWP panels (figure 2) will not be perfectly aligned (current target engineering maximum misalignment is $\sim$0.1 mm), heat loads will occur on the tile leading edges at near normal angles of incidence, increasing the tile edge temperature. Clearly, for a given radial misalignment, if a narrow feature is present, with elevated values of R_q, then the tile edge loading can be the limiting factor on FWP power handling, and not the surface load determined by the global shaping. However, if the misalignment does not exceed the current target engineering maximum, then ion Larmor radius 'smoothing' effects might somewhat reduce the perpendicular edge load due to ions [45, 46], particularly in limiter plasmas, where the edge ion temperatures are known to be high [47]. High T_i yields large ion Larmor radius and a stronger smoothing effect. The latter is in fact expected to be somewhat stronger for the new IW FWP toroidal shape which features smaller α_{inc} at the apex where the incident heat flux will be largest. It is clear that more theoretical and experimental study of this effect will be required in the future.

6.2. Heat load on the FWP poloidal edge at the toroidal shape transition

As mentioned in the introduction to this section, given that the proposed new toroidal shape comes at a late stage in the engineering design of the IW FWPs, it is a considerable simplification if the original logarithmic profile for NHF panels in poloidal rows 1, 2 and 6, 7 can be retained and the modification applied only to the EHF panels 3–5, the only units concerned by IW plasma start-up. Since the poloidal set-backs are the same for all IW FWPs (section 5), the new shape of FWPs 3–5 renders the lower poloidal edge of FWP 3 and the upper poloidal edge of FWP 5 potentially open to direct plasma exposure, depending on the equilibrium. Although it is not essential that the FWP poloidal edges are completely shadowed, it is important to verify that power loads in the case of edge exposure are less than some critical value. The latter is determined by an empirical criterion that the power incident on the FWP beryllium tile poloidal edge is $\lesssim$10% of the maximum power onto the entire tile face [23]. Mathematically, this may be written:

$$P_{edge} = L_{tile}\Delta_{pen}q_{surf\ edge} < P_{edge,max} = 0.1P_{face,max} = 0.1L_{tile}^2 \approx 68\text{W}, \quad (12)$$

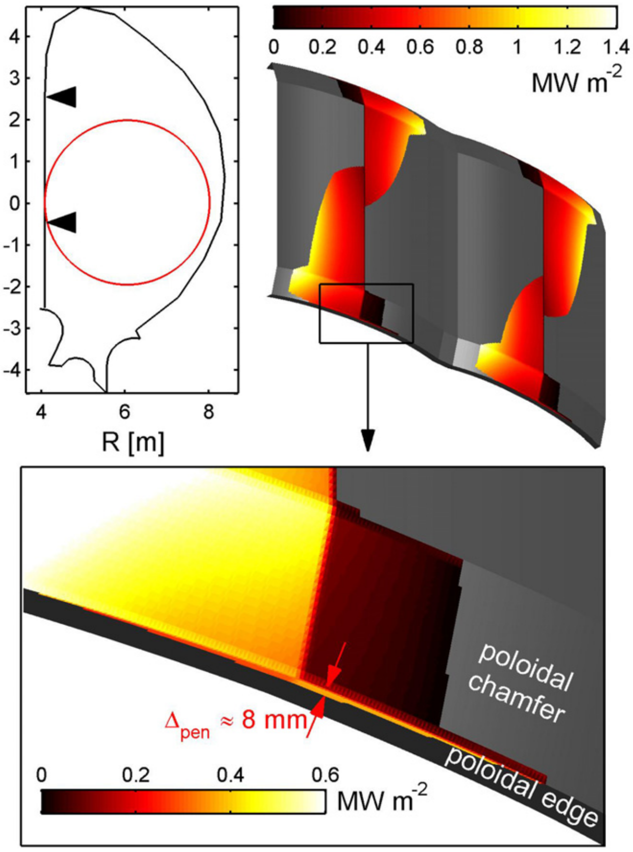

Figure 17. Example of the poloidal edge loading on FWP 3 observed for a circular IWL plasma ($a = 2$ m, $P_{\rm SOL} = I_{\rm p} = 5$ MA/MW, $\lambda_{\rm q,main} = 100$ mm) with contact point located ~0.5 m above the lower poloidal edge of FWP 3. Triangles in the poloidal plasma cross-section indicate the transitions in the IW FWP toroidal shape.

where $\Delta_{\rm pen}$ is the plasma penetration width on the tile poloidal edge, and $q_{\rm surf\ edge}$ is the corresponding surface heat load, averaged over the edge wetted area.

Several magnetic equilibria have been examined to study this edge loading in the case of modified toroidal shaping on FWPs 3–5, including those from the IW start-up sequence in figure 1, as well as somewhat artificial cases of a large ($\leqslant$2 m minor radius) IWL circular plasma characterized by $P_{\rm SOL} = I_{\rm p}$ up to 5 MW/MA. To study the sensitivity of $q_{\rm surf\ edge}$ to the plasma contact point position, the equilibria are shifted vertically around the nominal contact point within the limits dictated by the overall first wall contour. From this study it appears that the only situation in which poloidal edge exposure occurs is the case of a near circular plasma with a contact point far enough from the EHF to NHF panel transition for the field line incidence angle to be large enough to escape the next-poloidal-neighbour shadowing provided by $\Delta^{\rm pol}_{\rm set\text{-}back}$, but yet close enough for the poloidal edge to be exposed to appreciable $q_\parallel$.

Figure 17 illustrates the surface heat load distribution for the case of circular plasma with $P_{\rm SOL} = I_{\rm p} = 5$ MW/MA, $B_t = 5.3$ T, shifted downwards onto a 5 mm radially misaligned FWP 3 (to increase the likelihood of poloidal edge exposure) on which is imposed a single exponential heat flux profile with $\lambda_{\rm q,main} = 100$ mm (to maximize $q_\parallel$ on the exposed edge). This value of $\lambda_{\rm q,main}$ is a factor 2 higher than would be predicted by the multi-machine scaling [24] for $I_{\rm p} = 5$ MA.

The field line tracing yields $\Delta_{\rm pen} \approx 8$ mm and $q_{\rm surf\ edge} \approx 0.4$ MW m^{-2} so that $P_{\rm edge} \approx 35$ W. Figure 18 shows that $P_{\rm edge} < 0.5P_{\rm edge,max}$ when the variation of both $\lambda_{\rm q,main}$ and $\Delta z_{\rm contact}$ is considered. Interestingly, as shown in figure 17, $\Delta_{\rm pen}$ is largest near the toroidal location of the FWP apex. Since the apex radial and toroidal location is the same for both the original and modified FWP toroidal shapes (figure 9), $P_{\rm edge}$ would be actually very similar even if the EHF FWP toroidal shape were not changed. Finally it should be mentioned that although the focus here has been on the study of the loads on the lower poloidal edge of FWP 3, the same heat loads would be obtained on the upper poloidal edge of FWP 5 by shifting the plasma upwards.

7. Summary

In ITER, the IW and OW FWPs will serve as limiters during plasma start-up and termination. Start-up on the IW offers many important advantages compared with the LFS, even though scenario analysis in fact indicates that in the early current rise phase to a full bore limiter at a few MA of plasma current, it may not be possible to guarantee that the plasma is IW or OW limited at all times in ITER.

To avoid the exposure of edges to plasma flowing on field lines at grazing incidence, the ITER FWPs are toroidally shaped, with a shaping profile for the inner and OW modules designed to optimize power deposition for a SOL heat flux

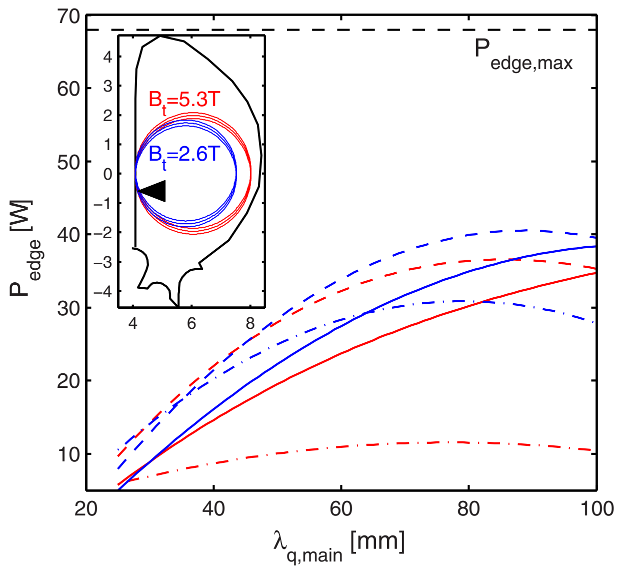

Figure 18. Power incident to a tile at the bottom poloidal edge of FWP 3 (marked by the triangle in the equilibrium reconstruction) as a function of $\lambda_{q,main}$, evaluated for plasma equilibria for which the largest poloidal edge loading is identified ($P_{SOL} = I_p = 5$ MW/MA, $B_t = 2.5$ and 5.3 T). $\Delta z_{contact} = -0.4$ m (full), -0.5 m (dashed) and -0.6 m (dashed–dotted). Horizontal dashed line indicates $P_{edge,max}$ from equation (12).

profile characterized by a single exponential decrease from the LCFS outwards. However, during limiter plasma experiments on JET executed in 2012 and designed to characterize the main SOL power width to consolidate the ITER design assumptions, high resolution IR measurements of power deposition on the tiles of an IW belt limiter found clear evidence for a very sharp feature ($\lambda_q \sim$ few mm, typically an order of magnitude smaller than the main SOL width) in the parallel heat flux profile in the near-SOL close to the LCFS. This is not the first time such a feature has been observed in limiter tokamaks (it was in fact first seen as early as the mid-1980s), but the earlier observations were not systematically pursued and, as this paper has discussed, their relevance to the ITER IWL is not entirely clear.

Following the new observation on JET and recognizing the potential importance for power handling on an ITER-like limiter with poorly adapted shaping, a new multi-machine study was initiated, eventually including five tokamaks, to understand both if the feature is universally present and, if so, to construct a physics basis suitable for extrapolation to ITER. This paper first summarizes the findings of this multi-machine study, where in fact the narrow feature has been clearly found in all cases. Generally these widths are found to scale with the ion poloidal gyro-radius and, surprisingly, to be consistent with λ_q measured in H-mode divertor plasmas. Key parameters are extracted to permit the derivation of a new toroidal shape for the ITER IW panels which mitigates the effect of the narrow SOL heat flux feature, should it be found on ITER. The new shape then used, in conjunction with three dimensional field line tracing on the ITER IW limiter panels, to demonstrate that for a wide variety of start-up equilibria and associated plasma parameters, and taking into account assembly tolerances, the power handling capability of the original shape design can be completely recovered in the presence of the projected narrow feature. Moreover, it is further shown that the new shape has the interesting property of both mitigating the impact of the narrow feature and resulting in only a modest increase in heat load, compared to the current design, if the narrow feature is not eventually found on ITER. The study has also clearly demonstrated that if the narrow heat flux feature were present in ITER and the IW toroidal profile is not modified accordingly, inboard limiter operation with plasma current up to several MA, as required by the ITER Heat Load Specifications, would not be possible.

As a result of this work, a new shape for the high heat flux panels in the start-up regions of the ITER IW has been proposed.

Acknowledgments

This work was supported in part by the US Department of Energy under DE-AC02-09CH11466, DE-FG02-94ER54235, DE-AC52-07NA27344 and DE-FC02-04ER54698 as and by the projects GA CR P205/12/2327 and MSMT LM2011021. This project has also received funding from the European Union's Horizon 2020 research and innovation programme under grant agreement number 633053.

The views and opinions expressed herein do not necessarily reflect those of the ITER Organization and of the European Commission.

References

[1] Mitteau R. *et al* 2010 *Fusion Eng. Des.* **85** 2049
[2] Pitts R.A. *et al* 2011 *J. Nucl. Mater.* **415** S957
[3] Raffray A.R. *et al* 2014 *Nucl. Fusion* **54** 033004
[4] Harbour P.J. and Loarte A. 1995 *Nucl. Fusion* **35** 759
[5] Gunn J.P. *et al* 2007 *J. Nucl. Mater.* **363–365** 484
[6] Kocan M. and Gunn J.P. 2010 *Plasma Phys. Control. Fusion* **52** 045010
[7] Rudakov D.L. *et al* 2011 *J. Nucl. Mater.* **415** S387
[8] Saoutic B. and The Tore Supra Team 2012 *Proc. 24th Int. Conf. on Fusion Energy (San Diego, CA, 8–13 October 2012)* www-naweb.iaea.org/napc/physics/FEC/FEC2012/index.htm
[9] Silva C. *et al* 2014 *Nucl. Fusion* **54** 083022
[10] Arnoux G. *et al* 2013 *Nucl. Fusion* **53** 073016
[11] Dejarnac R. *et al* 2015 *J. Nucl. Mater.* (http://dx.doi.org/10.1016/j.jnucmat.2014.12.100)
[12] Horacek J. *et al* 2014 *J. Nucl. Mater.* (http://dx.doi.org/10.1016/j.jnucmat.2014.11.132)
[13] Nespoli F. *et al* 2015 *J. Nucl. Mater.* (http://dx.doi.org/10.1016/j.jnucmat.2014.11.137)
[14] Stangeby P.C. *et al* 2015 *J. Nucl. Mater.* (http://dx.doi.org/10.1016/j.jnucmat.2014.09.051)
[15] Chankin A.V. *et al* 1987 *J. Nucl. Mater.* **145–147** 789
[16] Stangeby P.C. 1992 *Nucl. Fusion* **32** 2079
[17] Mitteau R. *et al* 1999 *Proc. 26th EPS Conf. on Controlled Fusion and Plasma Physics (Maastricht, Netherlands, 14–18 June 1999)* vol 23J (ECA) pp 1001–4 http://epsppd.epfl.ch/Maas/web/pdf/p3012.pdf
[18] Denner T. *et al* 1999 *Nucl. Fusion* **39** 83
[19] Finken K.H. *et al* 2000 *Nucl. Fusion* **40** 339
[20] Zweben S.J. *et al* 2009 *Phys. Plasmas* **16** 082505
[21] Lukash V.E. *et al* 2011 Simulation of ITER plasma scenarios starting from initial discharge of central solenoid *Proc. 38th EPS Conf. on Plasma Physics (Strasbourg, France, 2011)* P2.109 http://ocs.ciemat.es/EPS2011PAP/pdf/P2.109.pdf
[22] Mitteau R. *et al* 2013 *Fusion Eng. Des.* **88** 568
[23] Stangeby P.C. 2011 *Nucl. Fusion* **51** 103015

[24] Horacek J. *et al* 2014 Multi-machine scaling of main SOL parallel heat flux width in tokamak limiter plasmas, in preparation
[25] LaBombard B. and Lipschultz B. 1987 *Nucl. Fusion* **27** 81
[26] LaBombard B. *et al* 2004 *Nucl. Fusion* **44** 1047
[27] Erents S.K. *et al* 2004 *Plasma Phys. Control. Fusion* **46** 1757
[28] Pitts R.A. *et al* 2007 *J. Nucl. Mater.* **363–365** 505
[29] Mitteau R. *et al* 2015 *J. Nucl. Mater.* (http://dx.doi.org/10.1016/j.jnucmat.2014.12.102)
[30] LaBombard B. 2014 unpublished experimental data
[31] Becoulet A. *et al* 2013 *Nucl. Fusion* **53** 104023
[32] Eich T. *et al* 2013 *Nucl. Fusion* **53** 093013
[33] Goldston R.J. 2015 *J. Nucl. Mater.* (http://dx.doi.org/10.1016/j.jnucmat.2014.10.080)
[34] Goldston R.J. 2012 *Nucl. Fusion* **52** 013009
[35] Nedopasov A.V. and Petrov V.G. 1986 *Nucl. Fusion* **26** 1529
[36] Kobayashi M. *et al* 2007 *Nucl. Fusion* **47** 61
[37] Lunt T. 2014 unpublished EMC3 Eirene results
[38] Cohen R.H. and Ryutov D.D. 1995 *Phys. Plasmas* **2** 2011
[39] Stangeby P.C. 2012 *Nucl. Fusion* **52** 083012
[40] Chodura R. 1982 *Phys. Fluids* **25** 1628
[41] Holland D.L., Fried B.D. and Morales G.J. 1993 *Phys. Fluids B* **5** 1723
[42] Gunn J.P. *et al* 2013 *J. Nucl. Mater.* **438** S184
[43] Firdaouss M. *et al* 2013 *J. Nucl. Mater.* **438** S536
[44] Pitts R.A. *et al* 2013 *J. Nucl. Mater.* **438** S48
[45] Corre Y. *et al* 2014 *J. Nucl. Mater.* (http://dx.doi.org/10.1016/j.jnucmat.2014.10.036)
[46] Dejarnac R. *et al* 2014 *Nucl. Fusion* **54** 123011
[47] Kocan M. *et al* 2011 *J. Nucl. Mater.* **415** S1133